

NASA CR-168266
GTD 83-10

INVESTIGATION OF A
PULSED ELECTROTHERMAL THRUSTER

by R. L. Burton, S. A. Goldstein, B. K. Hilko,
D. A. Tidman, and N. K. Winsor

GT-DEVICES, INC.

prepared for

NATIONAL AERONAUTICS AND SPACE ADMINISTRATION

NASA Lewis Research Center
Contract NAS 3-23779

(NASA-CR-168266) INVESTIGATION OF A PULSED
ELECTROTHERMAL THRUSTER (GT-Devices) 45 p
HC A03/MF A01 CSCL 21C

N84-12227

Unclas
G3/20 42578

1. Report No. NASA CR-168266	2. Government Accession No.	3. Recipient's Catalog No.	
4. Title and Subtitle Investigation of a Pulsed Electrothermal Thruster		5. Report Date October 1, 1983	
		C Performing Organization Code	
7. Author(s) R. L. Burton, S. A. Goldstein, B. K. Hilko, D. A. Tidman, and N. K. Winsor		8. Performing Organization Report No. GTD Report No. 83-10	
9. Performing Organization Name and Address GT-Devices, Inc. 5705 General Washington Drive Alexandria, VA 22312		10. Work Unit No.	
		11. Contract or Grant No. NAS 3-23779	
12. Sponsoring Agency Name and Address National Aeronautics and Space Administration Washington, DC 20546		13. Type of Report and Period Covered Contract Report	
		14. Sponsoring Agency Code	
15. Supplementary Notes Project Manager, Shih-Ying Wang, Space Propulsion Technology Division, NASA Lewis Research Center			
16. Abstract Exhaust velocity and thrust measurements are performed on a Pulsed Electrothermal (PET) Thruster using polyethylene and Teflon propellants. The results verify theoretical predictions of equilibrium flow in the nozzle, resulting in substantial recovery of the energy of dissociation and ionization. The thruster is tested in an unsteady mode (15 μ sec current pulse and 15 cm discharge length) and in a quasi-steady mode (48 μ sec current pulse and 5 cm discharge length). All tests are run at 2 kJ. The exhaust velocity of the propellant mass exiting during the current pulse is measured with two types of time-of-flight probes, and the impulse bit is measured on a thrust stand. It is inferred from both theory and experiment that an additional amount of mass is exhausted after the pulse. The measured thrust to power ratio for polyethylene is $T/P = 0.10$ N/kW at 21 km/sec in the unsteady mode, and $T/P = .053$ N/kW at 27 km/sec in the quasi-steady mode, where the velocities are measured by the time-of-flight probes. For Teflon propellant, $T/P = .20$ N/kW at 15 km/sec (unsteady mode) and 0.090 N/kW at 20 km/sec (quasi-steady mode). The discharge pressure and temperature predicted by a computational model for polyethylene are consistent with the measured thrust and discharge resistance. The total measured propellant ablation is in excellent agreement with that given by the model, which predicts that about 2/3 of the mass is ablated during the current pulse and about 1/3 at later times. The computed sound speed for polyethylene is 9 km/sec, indicating that the exhaust plasma (27 km/sec) is highly supersonic.			
17. Key Words (Suggested by Author(s)) Electric Propulsion Electrothermal Thruster Thruster Performance		18. Distribution Statement Unclassified-Unlimited	
19. Security Classif. (of this report) Unclassified	20. Security Classif. (of this page) Unclassified	21. No. of Pages 40	22. Price*

* For sale by the National Technical Information Service, Springfield, Virginia 22161

TABLE OF CONTENTS

	<u>Page</u>
Title Page.	i
Table of Contents	ii
Summary	iii
I. INTRODUCTION.	1
II. DESCRIPTION OF PET THRUSTER OPERATION	3
III. DESCRIPTION OF EXPERIMENTAL APPARATUS	10
IV. EXPERIMENTAL RESULTS.	25
V. DISCUSSION OF RESULTS	28
VI. CONCLUSION.	39
VII. APPENDIX I-REPORT DISTRIBUTION LIST	40
VIII. REFERENCES.	43

SUMMARY

The PET Thruster is an electric propulsion device which consists of a capillary-shaped pressure chamber with electrodes at each end. The cathode end is closed, and the exhaust electrode (anode) incorporates a supersonic nozzle. The pressure chamber inner wall is lined with an easily ablated, low molecular weight material such as polyethylene or Teflon. The pressure chamber is a high strength dielectric, capable of withstanding plasma pressure pulses up to 10^4 atm. The high pressure develops a jet of high velocity plasma from the nozzle, which provides rocket thrust.

The electrical energy store consists of a high voltage capacitor or pulse forming network, capable of storing a few kilojoules at several kilovolts. The impedance of this source is matched to the discharge resistance R , for efficient coupling. A switch with resistance $R_s \ll R$ permits over 90% of the stored energy to be transferred to the discharge in a single pulse. The width of the current pulse is typically 10-100 μ sec, with a peak current in the 20-100 kA range. Terminal voltage is 3-10 kV, giving a peak power dissipation on the order of 100 MW.

During a current pulse, I²R heating in the discharge chamber creates a plasma which radiates as a black body to the wall. The wall material is evaporated and is heated to a temperature of a few eV. The chamber pressure is typically $\sim 10,000$ atmospheres, so that the plasma is highly collisional and optically thick. For steady conditions in the chamber, the pressure drives a steady plasma flow through the supersonic nozzle. Because of the high gasdynamic pressure this nozzle flow is predicted to be in equilibrium. Thus, the efficiency of the PET Thruster is expected to be high.

Exhaust velocity and thrust measurements described in this report are performed using polyethylene and Teflon propellants. The results verify the theoretical predictions of equilibrium flow in the nozzle, resulting in substantial recovery of the energy of dissociation and ionization. The thruster is tested in an unsteady mode (15 μ sec current pulse and 15 cm discharge length) and in a quasi-steady mode (48 μ sec current pulse and 5 cm discharge length). All tests are run at 2 kJ. The exhaust velocity of the propellant mass exiting during the current pulse is measured with two types of time-of-flight probes, and the impulse bit is measured on a thrust stand. It is inferred from both theory and experiment that an additional amount of mass is exhausted after the pulse. The measured thrust to power ratio for polyethylene is $T/P = 0.10$ N/kW at 21 km/sec in the unsteady mode, and $T/P = 0.53$ N/kW at 27 km/sec in the quasi-steady mode, where the velocities are measured by the time-of-flight probes.

For Teflon propellant, $T/P = .20$ N/kW at 15 km/sec (unsteady mode) and 0.090 N/kW at 20 km/sec (quasi-steady mode).

The discharge pressure and temperature are predicted by a computational model for polyethylene, and are consistent with the measured thrust and discharge resistance. The total measured propellant ablation is in excellent agreement with that given by the model, which predicts that about 2/3 of the mass is ablated during the current pulse and about 1/3 at later times. The computed sound speed for polyethylene is 9 km/sec, indicating that the exhaust plasma (27 km/sec) is highly supersonic.

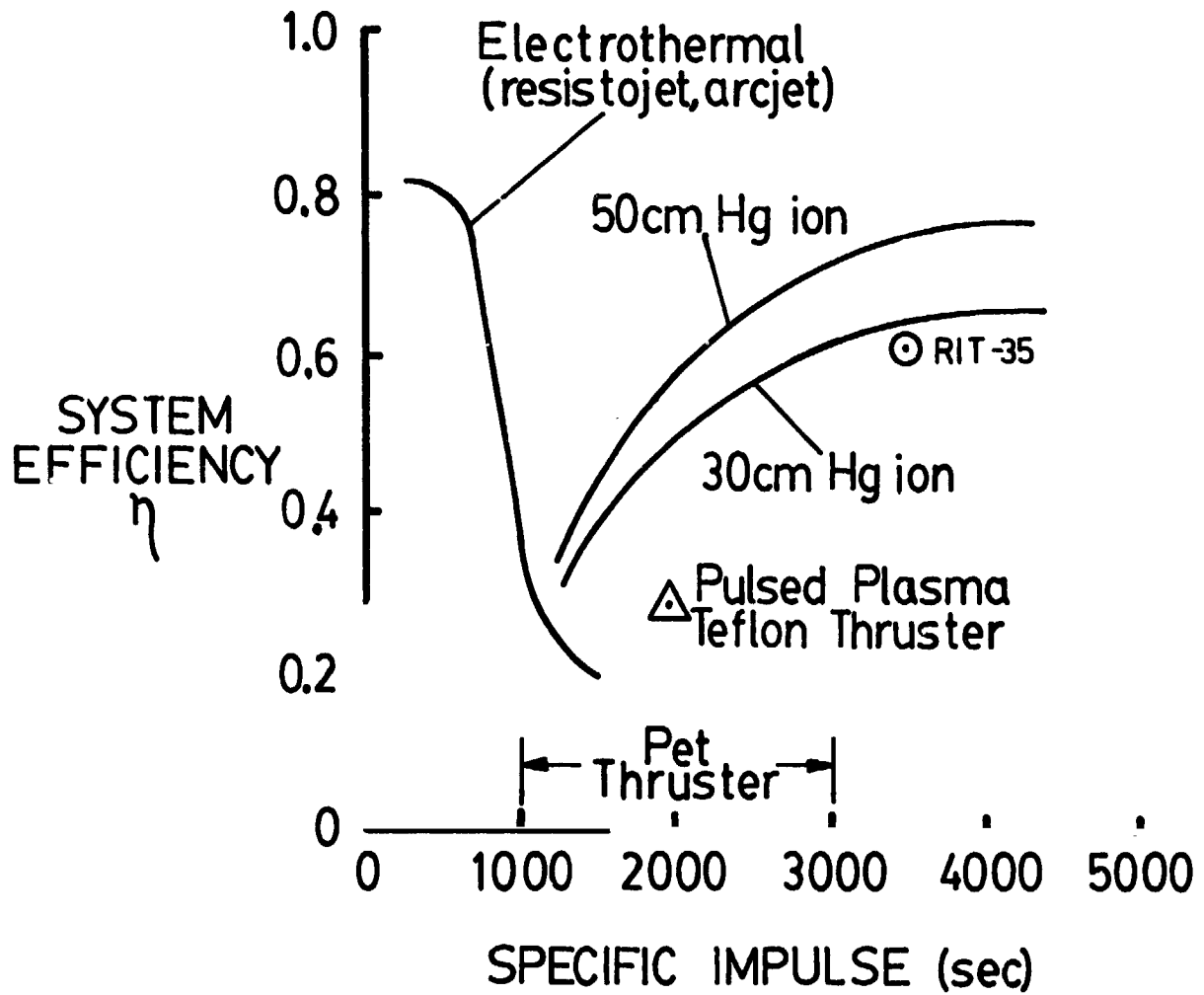
I. INTRODUCTION

After more than two decades of electric propulsion development, a requirement still remains for a system which has high efficiency in the 1000-2500 second specific impulse range. The problem is illustrated in Figure 1, which shows overall efficiency as a function of specific impulse for several electric propulsion systems.¹ Below 750 seconds and above 2500 seconds efficiencies exceeding 70% can be obtained, but in the intermediate range the efficiency of available systems falls as low as 30%.

The reason for the poor performance of these systems at 1000-2500 seconds is primarily the large internal energy of the exhaust flow, which is highly dissociated or ionized, representing a "frozen flow" energy loss which is not recoverable. Because the flow is frozen by the low number of recombination collisions, raising the flow density several orders of magnitude raises the collision rate to where most of the plasma internal energy can be recovered. In this report we present the results of the first thrust stand and exhaust flow tests of the PET (Pulsed Electro-thermal) Thruster, in order to check our prediction¹ of equilibrium flow in the nozzle. If true, equilibrium flow would permit efficient operation of the PET Thruster in the range of 1000-3000 seconds specific impulse.

Figure 1

ELECTRIC THRUSTER PERFORMANCE



II. DESCRIPTION OF PET THRUSTER OPERATION

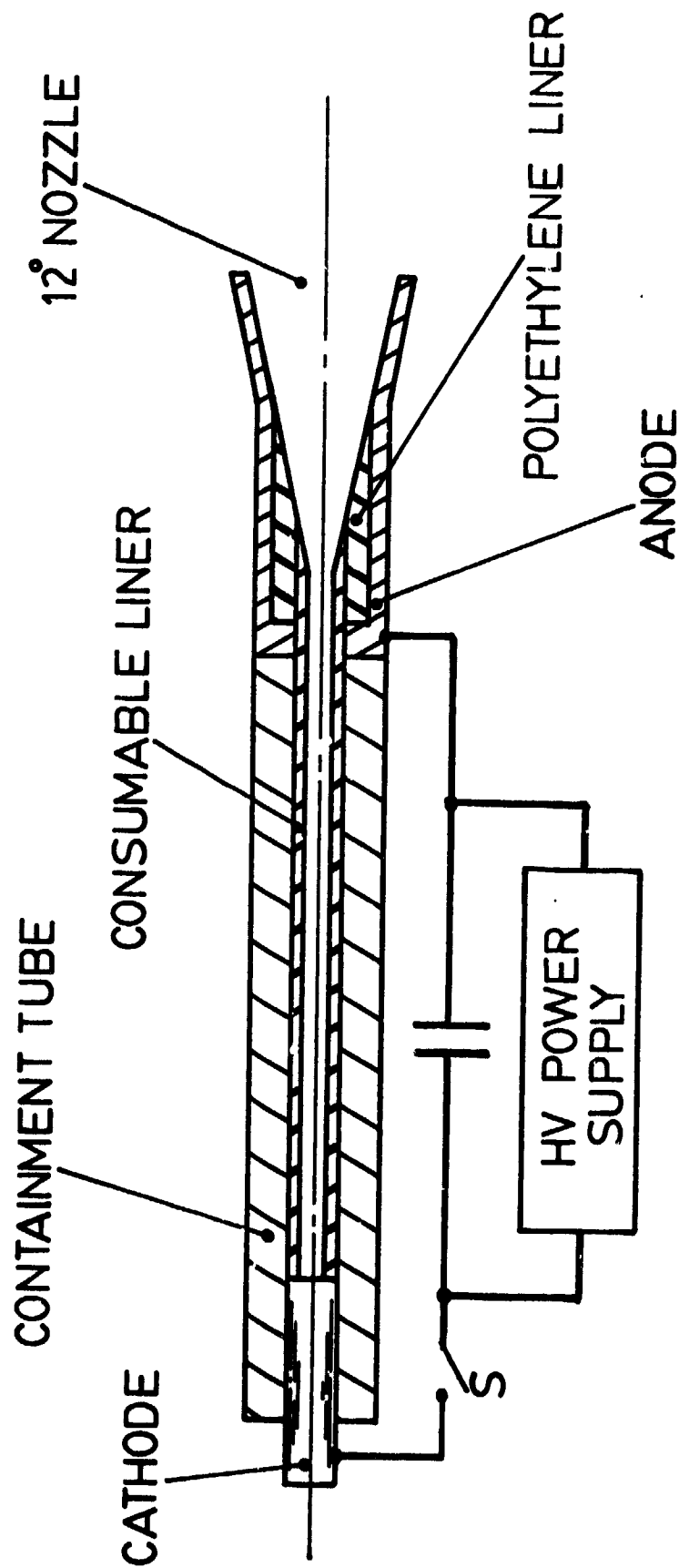
The PET Thruster (Figure 2) is an electric propulsion device which consists of a capillary-shaped pressure chamber with electrodes at each end. The cathode end is closed, and the exhaust electrode (anode) incorporates a supersonic nozzle. The pressure chamber inner wall is lined with an easily ablated, low molecular weight material such as polyethylene or Teflon. The pressure chamber is a high strength dielectric, capable of withstanding plasma pressure pulses up to 10^4 atm. The high pressure develops a jet of high velocity plasma from the nozzle, which provides rocket thrust.

The design of the thruster permits the propellant inner diameter and length to be changed easily for testing. The propellant can also be easily removed for weighing or replacement. The nozzle design places the anode downstream from the throat in a low-temperature region, which virtually eliminates erosion on this electrode.

The electrical energy store (Figure 2) consists of a high voltage capacitor or pulse forming network, capable of storing a few kilojoules at several kilovolts. The impedance of this source is matched to the discharge resistance R , for efficient

ORIGINAL PAGE IS
OF POOR QUALITY

Figure 2. PET THRUSTER SCHEMATIC



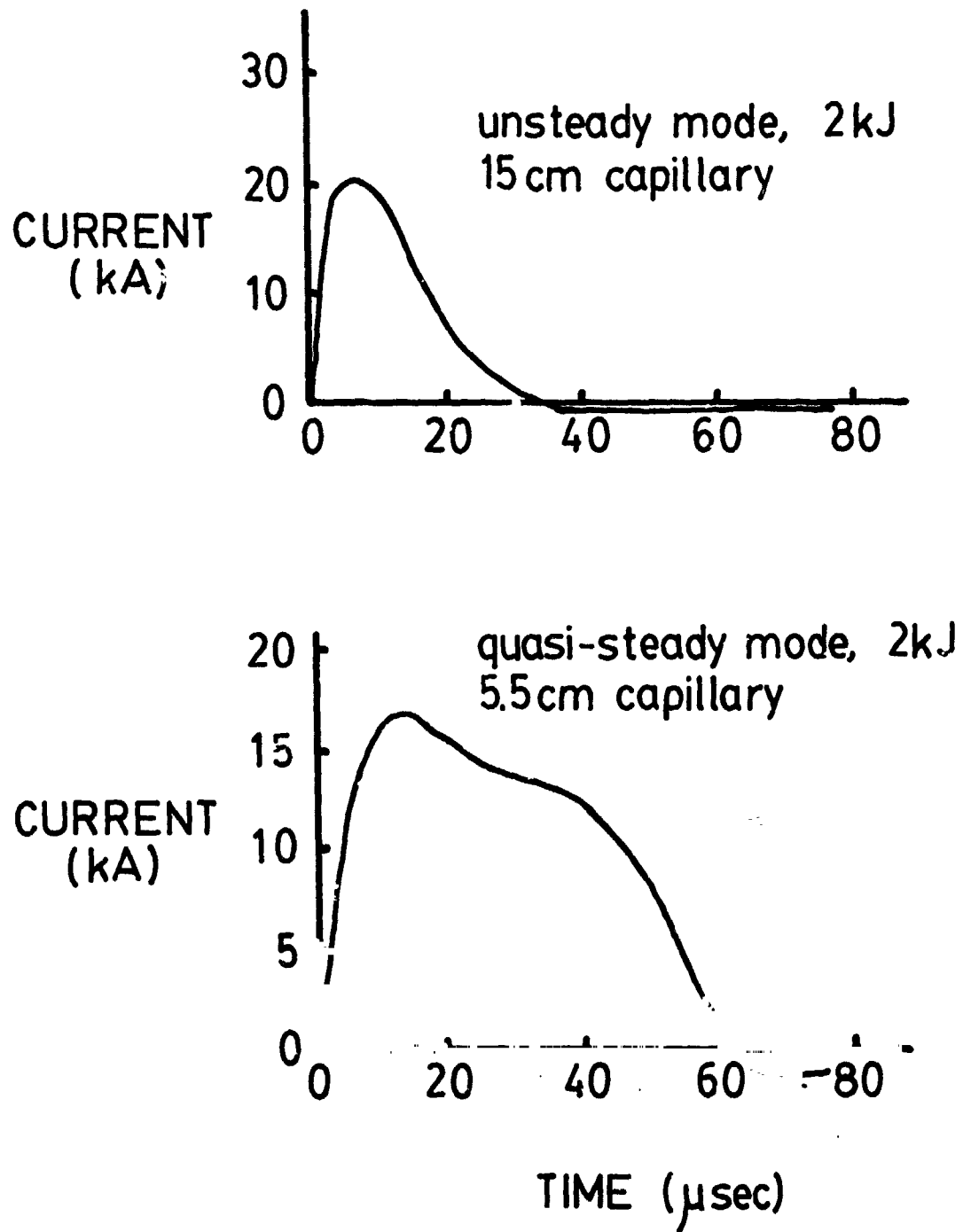
coupling. The switch (Figure 2) is an ignitron with resistance $R_s \ll R$, so that over 90% of the stored energy is transferred to the discharge in a single pulse. The width of the current pulse is typically 10-100 μ sec, with a peak in the 20-100 kA range. Terminal voltage is 3-10 kV, giving a peak power dissipation on the order of 100 MW.

It is possible to operate the PET Thruster in two modes, and results from both modes are presented in this report. The mode is determined by comparing the length of the current pulse, t_p , to the two-way longitudinal acoustic time in the capillary, $2\ell/c$. In the short pulse or unsteady mode, $t_{pc}/2\ell < 1$, and steady flow is not achieved through the nozzle. In the long pulse or quasi-steady mode, $t_{pc}/2\ell \gg 1$, and steady flow is achieved during the high current portion of the pulse. The 2 kJ tests described below result in higher specific impulse and efficiency for a PET Thruster operated in the quasi-steady mode. The two current pulses tested are shown in Figure 3.

Physics of Operation

The physics of the PET Thruster are most easily described for constant current operation.¹ Electrothermal heating in the discharge chamber at a rate I^2R creates a plasma which radiates as a black body to the wall. The wall material is evaporated and is heated to a temperature of a few eV. The chamber pressure is typically several thousand atmospheres, so that the plasma is

Figure 3
PET THRUSTER CURRENT WAVEFORMS



highly collisional and optically thick. For steady conditions in the chamber, the pressure drives a steady plasma flow through the supersonic nozzle. Because of the high gasdynamic pressure this nozzle flow is in equilibrium, as discussed below. Thus, the efficiency of the PET Thruster is expected to be high.

Nozzle Processes

Without an equilibrium flow nozzle, a highly ionized plasma exhaust would result in high frozen flow losses. At high densities, however, it appears that the ionization energy can be recovered. The three-body recombination rate is²

$$\nu_3 = 8.75 \times 10^{-27} T_{\text{eV}}^{-4.5} Z^3 n^2 (\text{cm}^{-3}) [\text{sec}^{-1}]$$

We can compare the collisional recombination time $1/\nu_3$, based on expected plasma conditions, to the nozzle flow time l/u_e . The smallest value of ν_3 occurs at the nozzle exit plane. For estimated values $T_{\text{eV}} = 0.5$ eV, $n_e = 2.5 \times 10^{18}$, $u_e = 2.5 \times 10^6$ cm/sec, and nozzle length $l = 10$ cm, $\nu_3 l/u_e \approx 2 \times 10^7$, so that recombination collisions are frequent in the nozzle. The flow expansion process therefore remains close to Saha equilibrium, and the ionization can be largely recovered.

Estimated Thrust Efficiency

We have tabulated the chemical bond energies for polyethylene,³ in order to estimate the thrust efficiency for equilibrium flow. The relevant energies for the production of six ions (2 carbon and 4 hydrogen) are summarized below:

evaporate C ₂ H ₄ from wall:	0.5 eV
break CC double bond	4.5 eV
break 4 CH bonds at 3.5 eV	14.0 eV

total for 6 ions	19.0 eV
evaporation and dissociation energy/ion	3.2 eV
mean ionization energy/ion	12.8 eV

total	16.0 eV/ion

We now use the Saha equation to estimate the degree of ionization at the exit plane. At low temperatures the Saha equation can be simplified to

$$\alpha = 3.11 \times 10^4 p^{-1/2} T_{\text{eV}}^{5/4} e^{-\epsilon_i/2T_{\text{eV}}}$$

where the pressure is in MKS units. For $p_e = 5 \times 10^4 \text{ N/m}^2$, $T_{ey} = 0.5 \text{ eV}$, $\epsilon_{diss} = 4.5 \text{ eV}$ and $\epsilon_i = 12.8 \text{ eV}$, the Saha equation predicts $\beta_{diss} = .65$ and $\alpha_{ion} = 1.6 \times 10^{-4}$. We can thus estimate the mean energy loss for the six ions as

loss from evaporation	0.5 eV/ion
loss from dissociation ($.65 \times 18.5/6$)	2.0
loss from ionization ($.00016 \times 12.8$)	0
loss from thermal ($3/2 T_{ey}$)	<u>.8</u>
$E_{loss} =$	3.3 eV/ion

The thruster efficiency for this example is then calculated from

$$\eta_T = \frac{\frac{1}{2}u_e^2}{\frac{1}{2}u_e^2 + eE_{loss}/m}$$

The mean ion molecular weight for polyethylene is 4.67. As an example, for $E_{loss} = 3.3 \text{ eV}$ and $u_e/g = 2500 \text{ seconds}$, $\eta_T = .82$.

III. DESCRIPTION OF EXPERIMENTAL APPARATUS

The performance of the PET thruster is measured on a simple linear thrust stand (Figures 4 and 5). The measurement is performed by freely suspending the thruster, firing it, and measuring the recoil velocity V . Knowing the recoil mass M , the impulse bit is measured by

$$\int T dt \text{ [N-s]} = MV$$

In order to insure that the thruster is freely suspended, the design of the thrust stand incorporates the following elements (see Figure 6).

1. The thruster mass (2.5 - 2.7 kg) is supported by a linear bearing which rolls on a horizontal hardened steel shaft. The center of gravity of the recoil mass lies directly on the thrust axis and in the vertical plane directly below the center of the bearing. Firing the thruster therefore produces simple linear motion with no binding of the bearing.

2. Current is fed into and out of the thruster through flexible strips of copper window screen (Figure 6). The strips are pie shaped with minimal gaps between the segments to minimize the fringing magnetic fields which could affect the diagnostics.

Figure 4. PET THRUSTER AND THRUST STAND



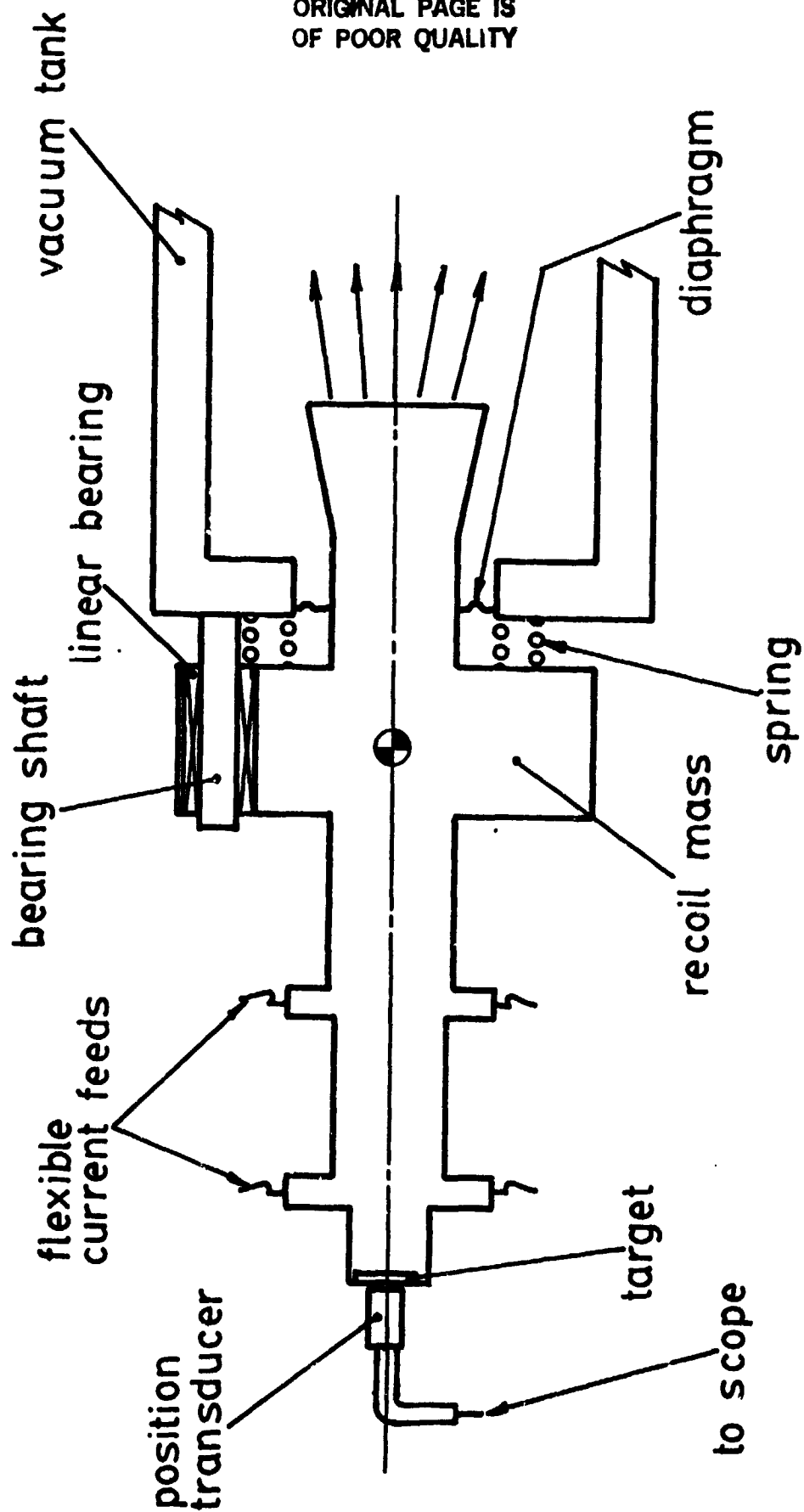
Figure 5. THRUST STAND AND VACUUM TANK

ORIGINAL PAGE IS
OF POOR QUALITY



ORIGINAL PAGE IS
OF POOR QUALITY

Figure 6
THRUST STAND SCHEMATIC



3. The thruster is sealed to the vacuum tank by a thin (0.4 mm) flexible diaphragm of rubber fabric, located at the nozzle throat (Figure 6). This arrangement keeps the electrical connections outside the vacuum tank, greatly simplifying the design of the high voltage insulation. The thruster and diaphragm must sustain a load caused by atmospheric pressure, and this load is counterbalanced by coil springs (Figure 6). The natural frequency of the thruster mass-spring system is 16 Hz, and the damping of the system is low, as is shown in the upper plot in Figure 7.

The recoil velocity is measured by a non-contact technique, using an inductive RF transducer⁴ coupled to an AISI 4142 steel target. The sensitivity of the transducer is 8V/mm, so that micron-level motions can be detected. The transducer output signal is recorded on a digital oscilloscope (Smartscope Model 3281) at 2 μ sec/point and is graphically differentiated to give V , the initial recoil velocity (Figure 8). Alternatively, the recoil velocity can be determined by fitting the output signal to a waveform $x(t) = x_0 e^{-\alpha t} \sin \omega t$, where α , x_0 and ω can be easily measured (Figure 7). Both techniques give equivalent results.

Delivered Energy

PET Thruster performance is based on the energy delivered to the discharge, determined by integration of the current and

Figure 7

THRUST STAND RESPONSE TO THRUST IMPULSE

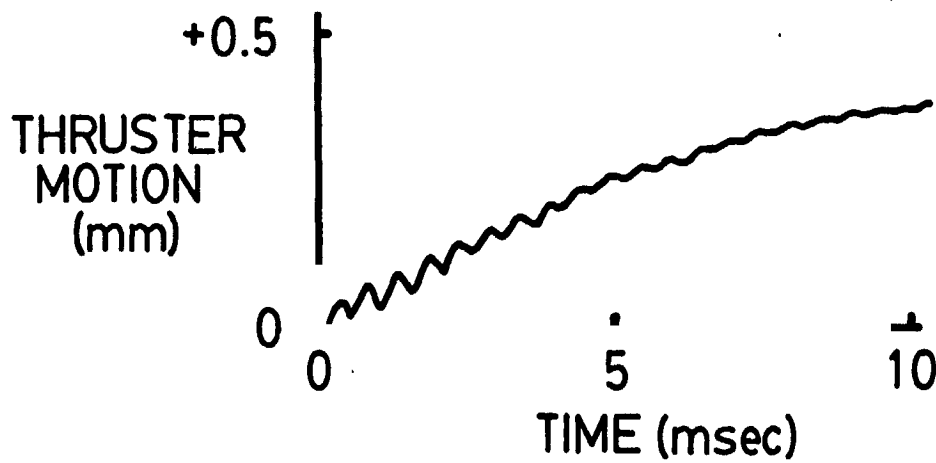
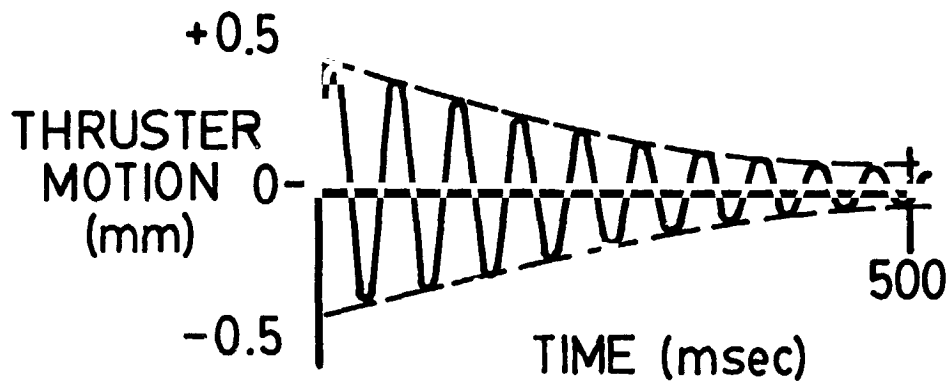
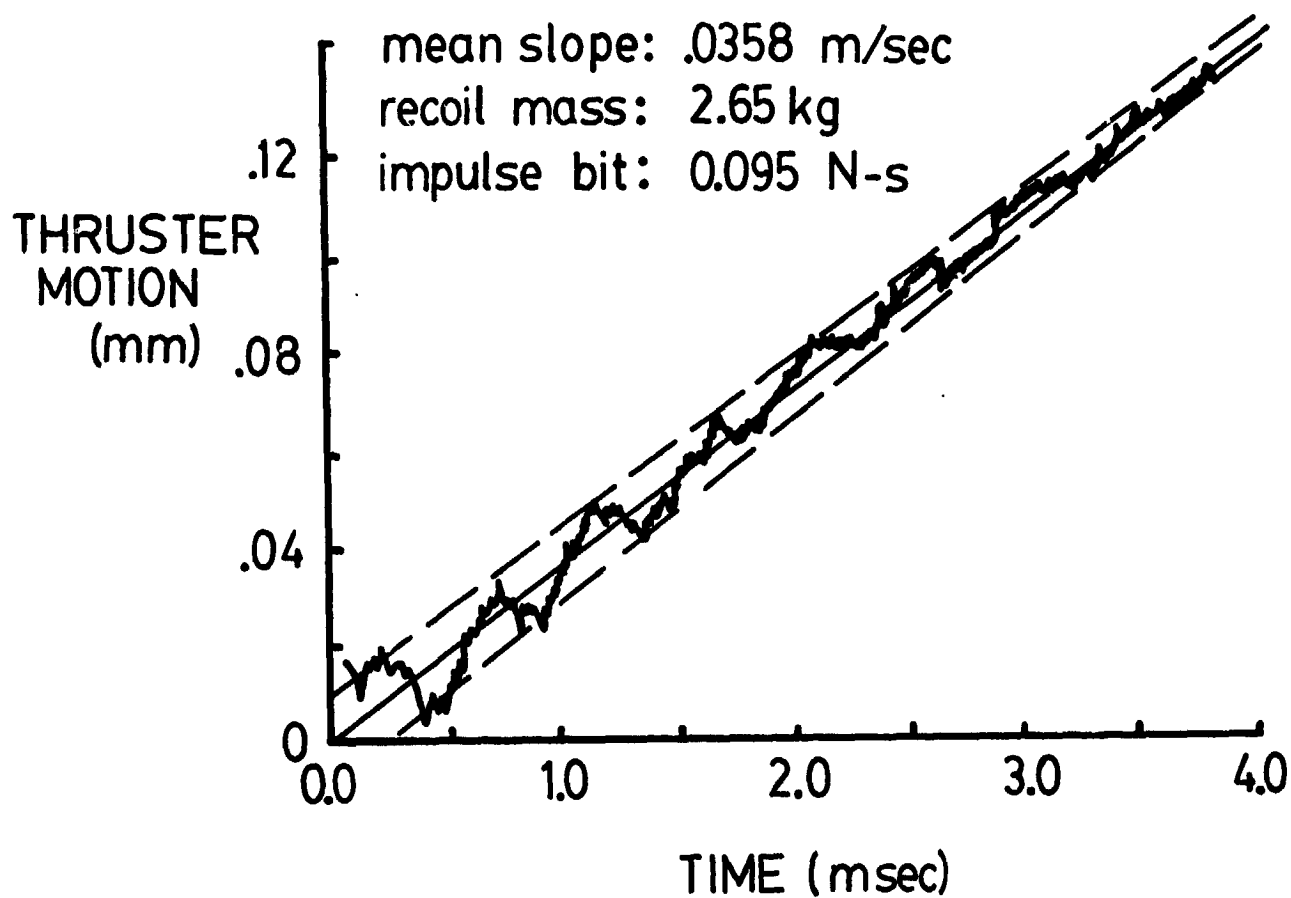


Figure 8

THRUST STAND MOMENTUM MEASUREMENT



voltage at the thruster terminals. Thruster current I is measured with a Rogowski loop, passively integrated with an $RC = 2.8$ msec integrator. Terminal voltage V is measured with a 935:1 resistive divider. Both I and V are recorded at $2\mu\text{sec/point}$, enabling the product IV to be internally computed, integrated, and displayed on the scopeface (Figure 9). The voltage is $V = IR + L_T \dot{I}$, where L_T is the inductance of the thruster. Thus,

$$\int IV dt = \int I^2 R dt + \frac{1}{2} L_T \int \frac{d}{dt}(I^2) dt$$

Denoting E_1 as the integral of the first half cycle, then

$$E_1 = \int IV dt = \int I^2 R dt = E_D \text{ [J]}$$

where E_D is the delivered energy. Because of the small external resistance, E_D is typically 92% of the stored energy.

Ablated Mass

The propellant ablated mass m is determined by a weighing procedure. The propellant is weighed on a sensitive scale (Volland Model 220R), and is weighed again after firing one or more shots. The cathode is weighed similarly. The nozzle is not weighed; however, visual inspection after 100 shots on the nozzle has shown no visible erosion.

Figure 9

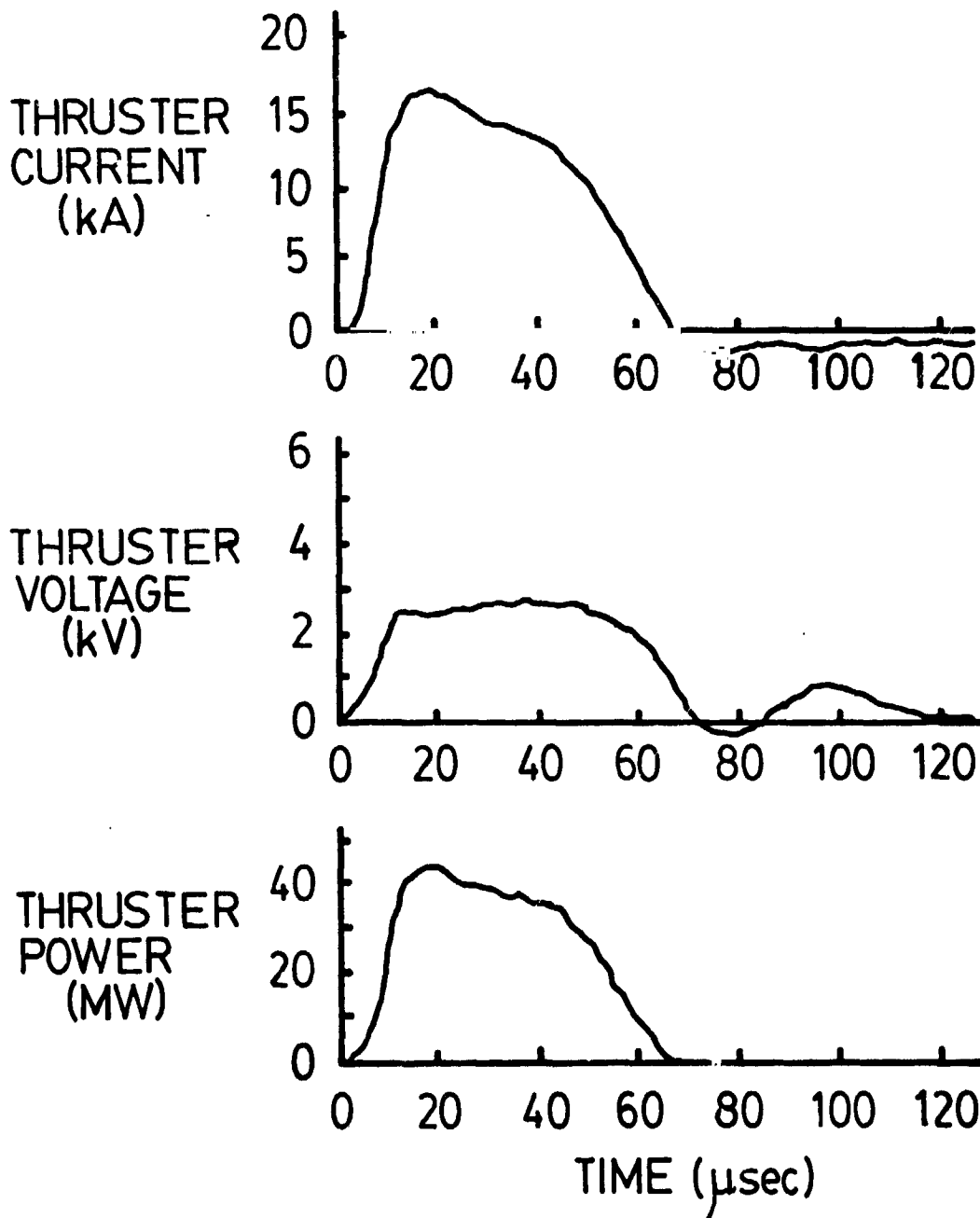
PET THRUSTER TERMINAL MEASUREMENTS

POLYETHYLENE PROPELLANT

5.5cm CAPILLARY

1.8kJ DELIVERED

ORIGINAL PAGE IS
OF POOR QUALITY



Exhaust Velocity

A number of techniques have been employed to measure exhaust velocity. These include a) an ion saturation probe, b) a piezoelectric stagnation pressure probe, and c) photodiode sensors, which record time of arrival of high velocity plasma at a stagnation point. The velocity measured by each of these techniques was generally in agreement. A description of each technique is presented below.

The ion saturation probe consists of 4 flush wires of 0.1 mm diameter mounted in a 90° epoxy cone. The wires are biased to -24V with an automotive lead-acid battery, referenced to the center electrode. When plasma arrives at the probe tip, a saturation current flows through the probe given by the saturation current density $j^+ = 1/4 n^+ e v_{th}^+$ flowing to the exposed area of the wires. Unfortunately this technique is unreliable, because the flush mounted wires become covered with material after a small number of shots, producing loss of signal. This covering is probably melted epoxy material from the probe tip.

The stagnation pressure probe (Figure 10) consists of a sensitive piezoelectric transducer (PCB 102A12, 44 psi/volt), mounted on the vacuum tank centerline on a moveable support. The transducer tip is covered with mylar tape for protection from the discharge. Typical probe signals are shown in Figure 11 for two

Figure 10

EXHAUST VELOCITY PROBES SCHEMATIC

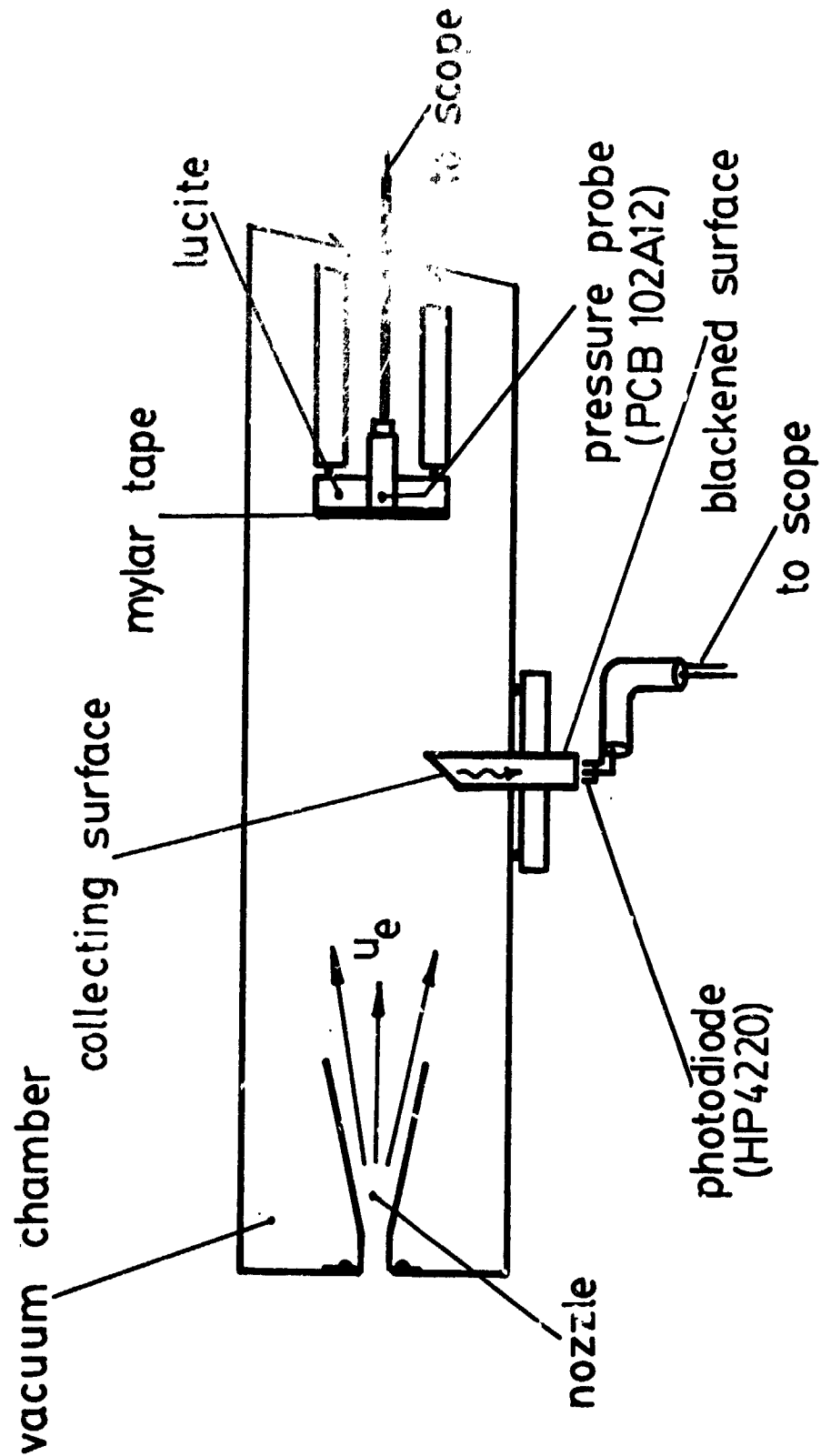
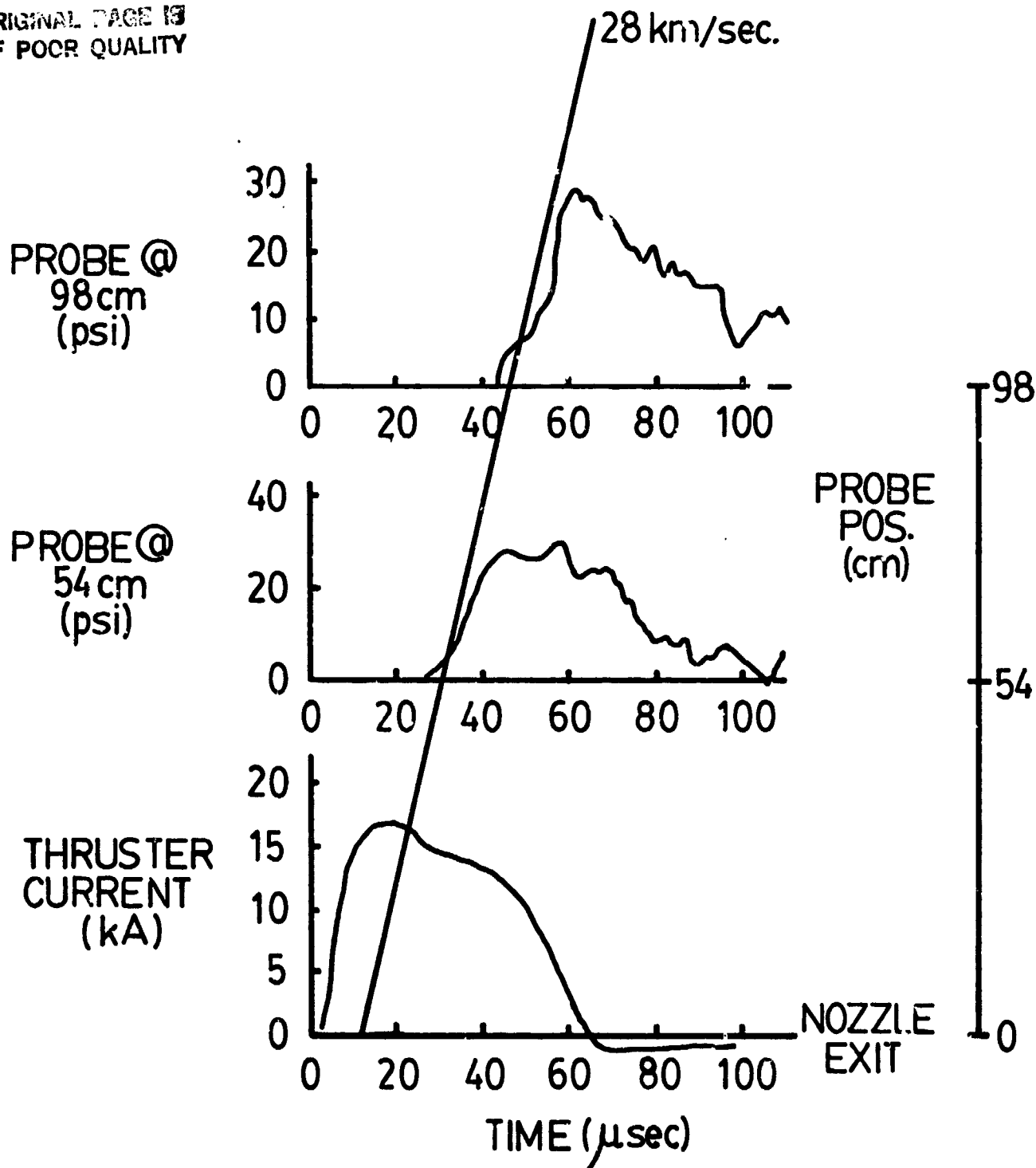


Figure 11

PRESSURE PROBE RESPONSE vs POSITION

POLYETHYLENE
5.5 cm CAPILLARY
1.8 kJ DELIVERED

ORIGINAL PAGE IS
OF POOR QUALITY



probe positions, showing that a time-of-arrival can be clearly measured for each shot. These times are then plotted, and the mean slope is measured graphically to determine the exhaust velocity.

A third time-of-arrival technique employs simple red-sensitive diodes to record the plasma flash on the tip of a transparent plastic stinger (Figure 10). The probe is located downstream from the nozzle exit plane and records a spike of radiation when fast moving plasma strikes the probe (Figure 12). Again, the arrival times for different axial probe positions are plotted to determine the exhaust velocity.

Because the total mass of the ambient gas in the tank at $P_{amb} \sim .003$ torr is a small fraction of the exhaust mass Δm , both the pressure transducer and the photodiode probes can be expected to respond to the exhaust mass without interference of the background gas. The data from the photodiode probe predicts velocities consistent with the data from the pressure transducer. Typical arrival time data, and the graphical measurement of exhaust velocity, is shown for both probes in Figure 13.

Figure 12

PHOTODIODE PROBE RESPONSE vs POSITION

POLYETHYLENE
5.5cm CAPILLARY
1.8 kJ DELIVERED

ORIGINAL PAGE IS
OF POOR QUALITY

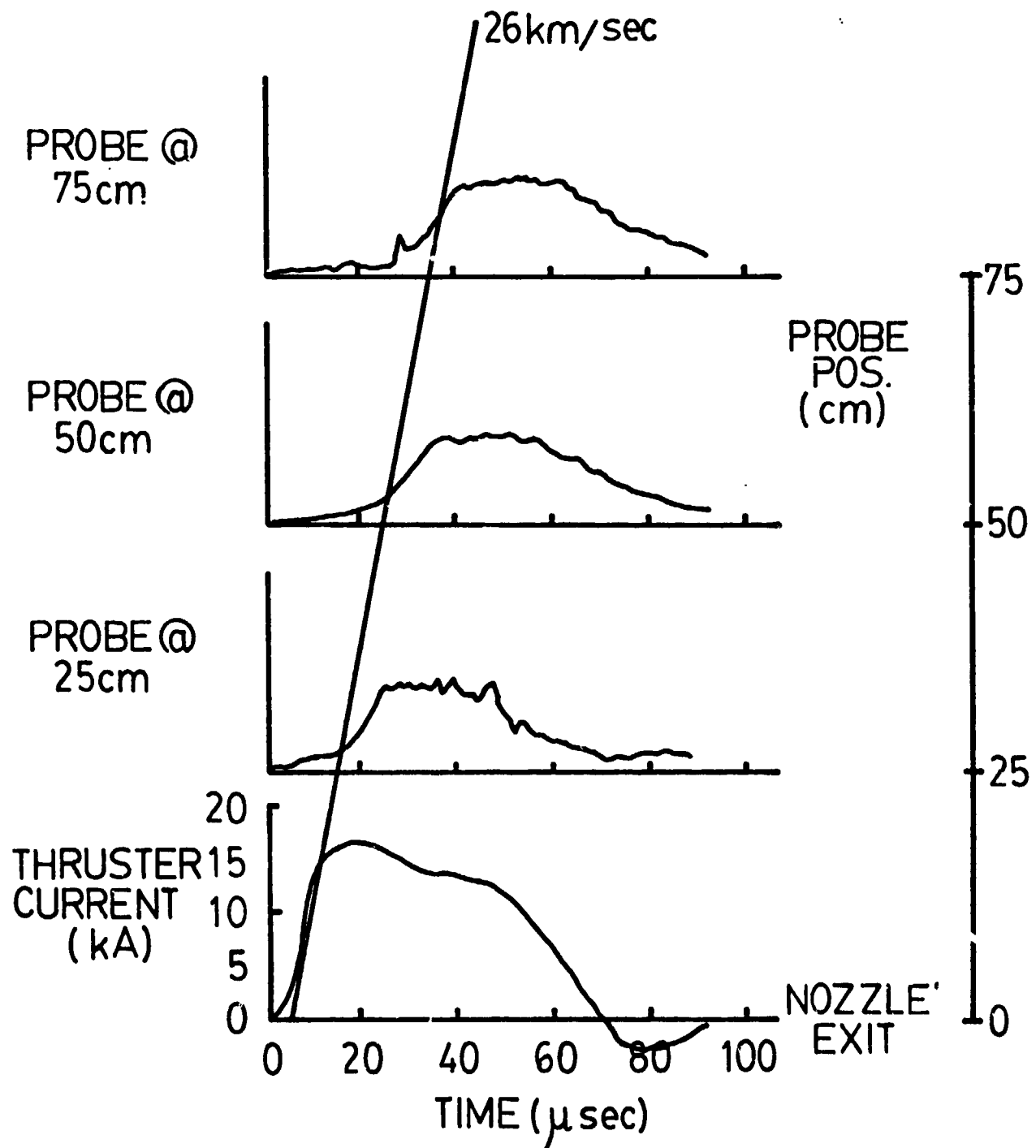


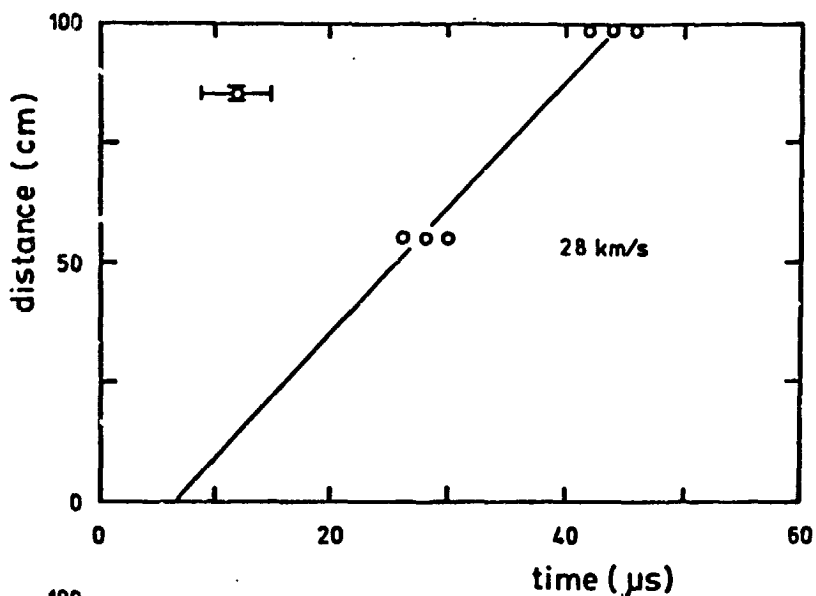
Figure 13

PET THRUSTER EXHAUST PROBE DATA

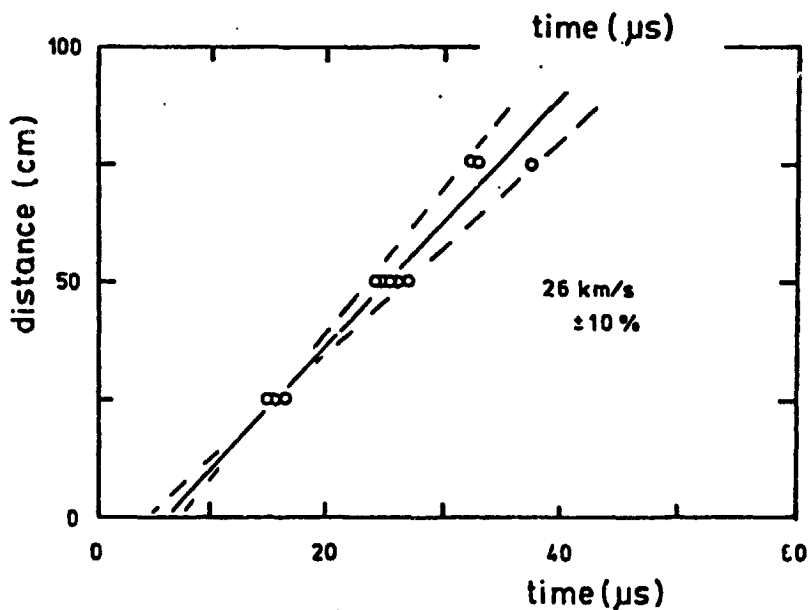
ORIGINAL PAGE 19
OF POOR QUALITY

polyethylene propellant
quasi-steady mode
1.8kJ delivered

PRESSURE
PROBE



PHOTODIODE
PROBE



IV. EXPERIMENTAL RESULTS

Two separate sets of tests were run on the PET Thruster, using two different current pulse waveforms (Figure 3). The first set of tests was run in the unsteady (short pulse) mode for which the thruster was driven by two 29 μ fd capacitors. Because of the high plasma resistance (0.2Ω), approximately 92% of the stored energy is transferred to the discharge chamber.

The second set of tests was run in the quasi-steady mode, for which the PET Thruster is driven by a broad current pulse, of 48 μ sec duration, (Figure 3). The pulse was again switched by an ignitron. The propellant chamber used in the quasi-steady mode is 5.5 cm long with a minimum resistance of $.160\Omega$, so that 90% of the stored energy is transferred.

The test plan calls for a ten-shot series with each propellant, polyethylene and teflon, so that 20 shots were run in the unsteady mode. An additional shorter series of shots was run in the quasi-steady mode. The data recorded, and the estimated precision of the measurements are:

- (1) recoil motion $x(t)$. Impulse bit is measured to 5%.
- (2) Exhaust probe time-of-flight, accurate to 10%.
- (3) I , accurate to 3%.
- (4) V , accurate to 3%.
- (5) Mass loss Δm , accurate to 6%.

The basic data are shown below in Table III and Table IV as averages for each series. These results are analyzed in the next section.

Table III. PET THRUSTER PERFORMANCE - UNSTEADY MODE,
15 CM CAPILLARY

	Polyethylene	Teflon
Delivered energy, E_D	1.80 kJ	1.87 kJ
Maximum current, I_M	23 kA	22 kA
Pulse width, half maximum	15 μ sec	15 μ sec
Thrust impulse bit, $\int T dt$.20 N-s	.35 N-s
Exhaust velocity		
Pressure transducer	21 km/s	15 km/s
Photodiode	20 km/s	14 km/s
Ablated mass, capillary only	20 mg/shot	117 mg/shot

Table IV. PET THRUSTER PERFORMANCE-QUASI-STEADY MODE,
5.5 CM CAPILLARY

	Polyethylene	Teflon
Delivered Energy, E_D	1.78 kJ	1.89 kJ
Maximum current, I_M	17 kA	12 kA
Pulse width, half maximum	48 μ sec	48 μ sec
Thrust impulse bit, $\int T dt$.095 N-s	.17 N-s
Exhaust velocity		
Pressure transducer	28 km/s	20 km/s
Photodiode	26 km/s	20 km/s
Ablated mass, capillary only	6.5 mg/shot	27 mg/shot

V. DISCUSSION OF RESULTS

At our present level of understanding and interpretation of the data, the results presented above in Tables III and IV should be interpreted cautiously. The thrust stand response, while highly repeatable, has not as yet been checked with an independent calibration procedure. Further uncertainty exists in the interpretation of the exhaust velocity and ablated mass measurements, as discussed below.

The thrust stand was designed as an oscillating spring-mass system with low damping, and this goal has been achieved, as shown in the slowly decaying sinusoidal thrust stand response in Fig. 7. Confidence in the accuracy of the thrust stand results is based on this low damping, and on the repeatability of the measurements of slope at $t = 0$. The raw impulse bit data for the 2 kJ tests presented in Tables III and IV is shown in Table V below. These results show that the thruster is operating repeatably, and that the measurement of the thruster recoil velocity does not introduce appreciable uncertainty into the final result.

Table V. PET THRUSTER IMPULSE BIT DATA, 2 kJ SHOTS

A. Polyethylene, 15 μ sec pulse B. Polyethylene, 48 μ sec pulse

$\int Tdt = .184$ N-s

.184
.190
.198
.205
.199
.204
.195
.194
.193

Mean .195 $\pm .007$ N-s

$\int Tdt = .094$ N-s

.0965
.0966
.0940
.0946
.0967
.0958

Mean .0954 $\pm .0014$ N-s

C. Teflon, 15 μ sec pulse

$\int Tdt = .373$ N-s

.340
.315
.406
.368
.350
.334
.400
.335
.311

Mean .353 $\pm .033$ N-s

D. Teflon, 48 μ sec pulse

$\int Tdt = .169$ N-s

.170
.169
.159

Mean .167 $\pm .005$ N-s

The measurement of exhaust velocity gives results which are consistent with our understanding of the physics of the discharge. In the unsteady mode case (Table III), the current impulsively heats the discharge plasma which is then accelerated as the temperature decays. The measured exhaust velocities are 20-21 km/sec for polyethylene and 14-15 km/sec for Teflon. The quasi-steady case (Table IV) achieves nearly steady state conditions, and hence a higher mean sound speed for the duration of the pulse. The exhaust velocities are correspondingly higher: 26-28 km/sec for polyethylene and 20 km/sec for Teflon. The ratio of exhaust velocity for polyethylene is about 1.4 that of Teflon, primarily due to Teflon's higher molecular weight.

What evidence do we have that the exhaust velocities measured correspond to electrothermally heated and accelerated propellant mass, and not to some relatively low mass precursor or shock wave? First is the time response of the pressure and photodiode probes (Figs. 11 and 12), which display a pulse width about equal to that of the current pulse. This suggests that the probe is responding to the momentum flux generated in the nozzle. Second is the nearly comparable velocity measured by the pressure and photodiode probes (Fig. 13); the latter responding to the radiation emitted by exhaust mass stagnating on a blunt body in the exhaust stream. Third, we have a theoretical prediction of the exhaust velocity, described in the next section, which gives reasonably good agreement with the measured values.

Computational Model

The predicted performance of a PET Thruster capillary with polyethylene can be modeled numerically.¹ Inputs to the GT-Devices code include polyethylene chemistry,⁵ plasma resistivity, capillary geometry, and the experimentally measured current and voltage waveforms. Because the plasma resistance is known, this can be used to calibrate the resistivity model used in the code, with the result that the plasma resistivity is close to that given by the Spitzer model.⁶ Predicted performance curves for a polyethylene 2 kJ shot in the quasi-steady mode are shown in Figure 14, which shows the capillary pressure, temperature and sound speed. The sound speed c_0 in the capillary is 8.5 km/sec during the current pulse, during which time $\gamma \approx 1.2$. Assuming adiabatic flow, with constant $\gamma = 1.2$ in the nozzle, the exit Mach number is then $M \sim 4.7$, corresponding to the nozzle area ratio of 95. At this Mach number the temperature drops by a factor:⁷

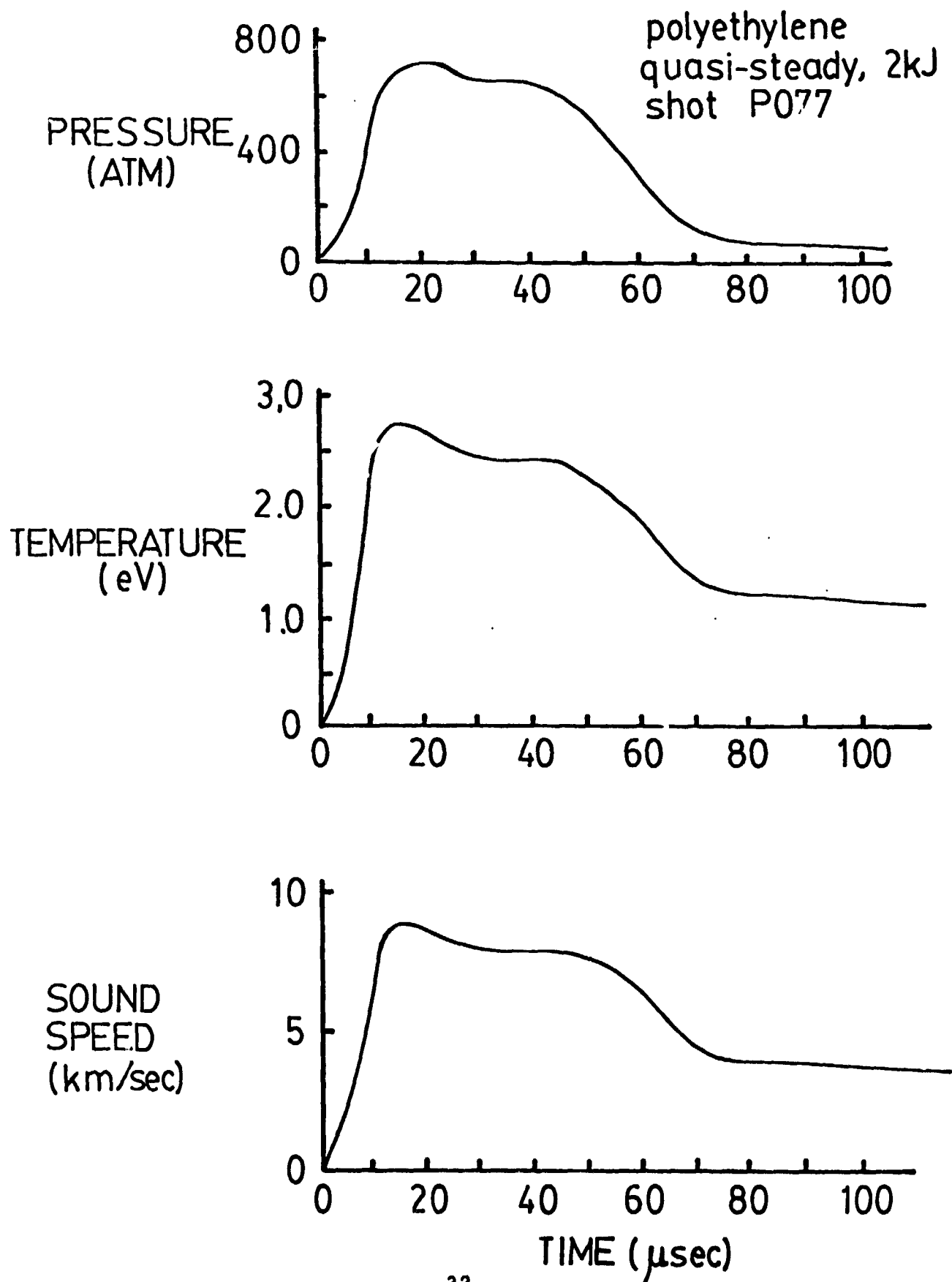
$$\frac{T_{ev}}{T} = 1 + \frac{\gamma-1}{2} M^2 = 3.2$$

The sound speed thus drops by a factor $\sqrt{3.2} = 1.8$, to $c = 4.8$ km/s. The exhaust velocity is then $u_e = Mc = 22$ km/sec, approximately the measured exhaust velocity.

More evidence for high Mach number flow lies in the pressure probe response (Fig.11), which shows a maximum signal of about 2

Figure 14

COMPUTED CAPILLARY PERFORMANCE



atmospheres. The thruster stagnation pressure can be estimated from the measured impulse bit, throat area, and pulse length⁷ as

$$p_0 \sim \frac{\int T dt}{C_F A^* t_p} \sim 710 \text{ atm}$$

for $C_F \sim 2$ and $t_p \sim 50 \mu\text{sec}$. This pressure is in agreement with that predicted by the computational model (Fig. 14). If we assume that a normal shock sits on the pressure probe tip, then in the limit $M^2 \gg (\gamma-1)/(\gamma+1)$ the probe response p_{oy} to the shocked gas is given by⁷

$$\frac{p_0}{p_{oy}} = \frac{\left(1 + \frac{\gamma-1}{2} M^2\right)^{\frac{\gamma}{\gamma-1}}}{M^2}$$

The probe peak amplitude of 2 atm corresponds to $p_{oy} \approx 350$. For $\gamma = 1.2$, this pressure ratio indicates $M \sim 6.3$, corresponding to a flow velocity of 24 km/sec for $c_0 = 8.5 \text{ km/sec}$. This value is consistent with the exhaust probe time-of-flight measurements.

Based on the numerical model, the measured exhaust velocities are consistent with a highly supersonic, adiabatic nozzle. Consistent with this model, the pulse width detected by the pressure transducer (Fig. 11) remains roughly constant with distance from the nozzle. This non-dispersive feature is characteristic of a high velocity puff of gas with a low sound speed. Furthermore, the measured velocity is consistent with adiabatic expansion of a polyethylene plasma with a stagnation temperature of 2.5 eV and a stagnation pressure of 10^3 atmospheres. The

stagnation enthalpy is 340 kJ/gram for polyethylene plasma,⁵ which would then fully expand to 26 km/sec. This value is close to those measured by the velocity probes.

Thrust to Power Ratio

The thrust to power ratio [N/kW] can be evaluated in the form

$$\frac{T}{P} \text{ [N/kW]} = \frac{\int T dt}{\int P dt / 1000} = \frac{\int T dt}{E_D \text{ [kJ]}}$$

The values of T/P for the 2 kJ shots (Tables III and IV) are shown below in Table VI. The velocities shown are those measured by the velocity probes for the mass exhausted during the current pulse.

Table VI. THRUST TO POWER RATIO FOR 2 kJ PULSES

	Polyethylene	Teflon
Unsteady,	.10 N/kW	.20 N/kW
15 μ sec pulse	@21 km/sec	@15 km/sec
Quasi-steady,	.053 N/kW	.090 N/kW
48 μ sec pulse	@27 km/sec	@20 km/sec

ORIGINAL PAGE IS
OF POOR QUALITY

For the quasi-steady case, these T/P values can be used to infer a thruster efficiency, as discussed below.

Thruster Efficiency

The thruster efficiency η_T is conventionally defined as

$$\eta_T = \frac{\text{exhaust kinetic energy}}{\text{energy delivered}} = \frac{\frac{1}{2} m u_e^2}{E_D}$$

For a pulsed device, the exhaust kinetic energy is

$$\frac{1}{2} m u_e^2 = \int \frac{1}{2} \dot{m} u_e^2 dt$$

where the integral is continued past the end of the current pulse length t_p to account for the discharge afterglow, during which propellant evaporation decays to zero. If the PET Thruster is operating in a purely steady mode, the efficiency can be found from u_e and T/P by

$$\eta_T = \frac{1}{2} u_e \frac{T}{P}$$

Using this efficiency and the measured u_e the energy loss per particle can be estimated from the equation for η_T given in section II above.

Thus the quasi-steady data in Table VI would predict:

Polyethylene, 27 km/sec $\eta_T = .72$ $E_{loss} = 6.9\text{eV}$

Teflon, 20 km/sec $\eta_T = .90$ $E_{loss} = 3.7\text{eV}$

While these numbers are certainly encouraging, they tend to overstate the efficiency, because the mass exhausted after the pulse at low velocity is not included in the calculation. As a check on the post-pulse mass ablation and on the quasi-steady nature of the discharge, we refer to the ablated mass measurements in Table IV. These mass measurements can be used to define a time-averaged exhaust velocity \bar{u}_e by

$$\bar{u}_e = \frac{1}{\Delta m} \int T dt$$

The values of u_e and \bar{u}_e for the quasi-steady data are shown in Table VII.

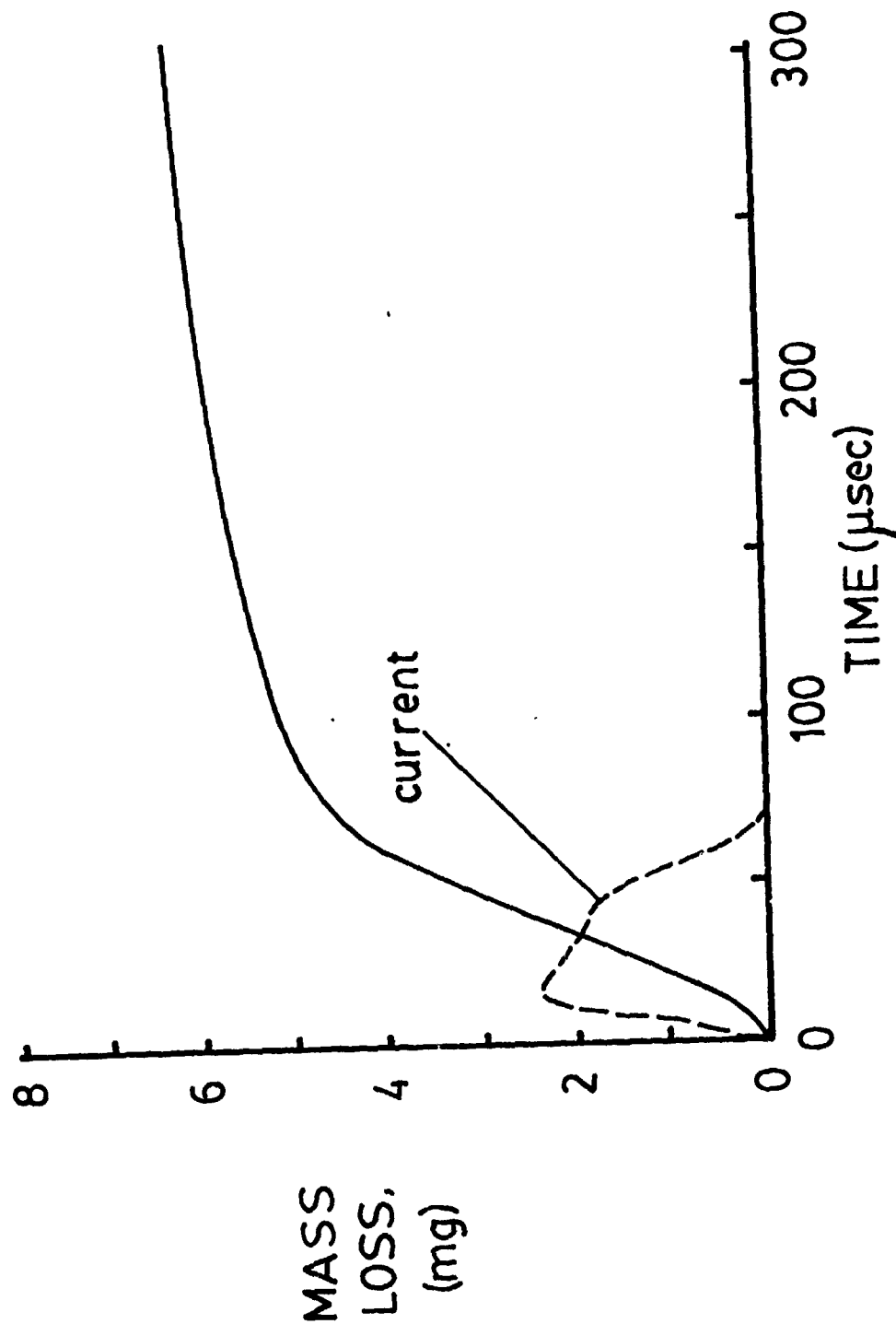
Table VII. MEASURED u_e AND PULSE-AVERAGED \bar{u}_e ,
QUASI-STEADY MODE

	Polyethylene	Teflon
Measured u_e	27 km/sec	20 km/sec
Mean $\bar{u}_e = \frac{1}{\Delta m} \int T dt$	15 km/sec	6 km/sec

The values in Table VII indicate that the thruster operation cannot be regarded as purely quasi-steady. We may postulate that the thruster operates in a quasi-steady mode during the high current portion of the current pulse, but departs from quasi-steady operation significantly during the fall and afterglow portions of the pulse. The net effect is to reduce the overall thruster efficiency for the pulse.

An estimate of the ablated mass time history is given by the computational model for a 2 kJ shot with polyethylene in the quasi-steady mode (Figure 15). The model predicts a total ablated mass of 6.2 mg, in excellent agreement with the average measured value of 6.5 mg per pulse. At the end of the current pulse, however, the model predicts that only 4.1 mg has been ejected. A significant fraction is thus exhausted at a much reduced velocity characteristic of the low temperature afterglow.

Figure 15
COMPUTED CAPILLARY MASS LOSS
polyethylene
quasi-steady, 2kJ
shot P077



VI. CONCLUSION

A PET Thruster has been built and tested on a thrust stand, giving repeatable results over a series of shots. Exhaust velocities for polyethylene and Teflon propellants in the quasi-steady mode of operation are 27 km/sec and 20 km/sec, as measured by exhaust probes. These velocities are consistent with computational predictions for these materials, assuming an adiabatic expansion to high Mach number in the conical nozzle. The performance data should be regarded cautiously, however, particularly with respects to the calculation of thruster efficiency. Future experiments are planned which provide for impulsive calibration of the thrust stand, and for determination of the mass flow time history in order to provide a clear interpretation of the efficiency data.